

- 285 (1993). For data in the Southern Hemisphere, see G. L. Maclean, *Cimbebasia* 2, 163 (1974); D. Robinson, *Emu* 90, 40 (1990); and R. E. Major, *Emu* 91, 236 (1991).
5. A. F. Skutch, *Ibis* 91, 430 (1949).
 6. T. H. Clutton-Brock, *The Evolution of Parental Care* (Princeton Univ. Press, Princeton, NJ, 1991).
 7. I. Rowley and E. Russell, in *Bird Population Studies: Relevance to Conservation and Management*, C. M. Perrins, J.-D. Lebreton, G. J. M. Hiron, Eds. (Oxford Univ. Press, Oxford, 1991), pp. 22–44.
 8. T. E. Martin, *J. Avian Biol.* 27, 263 (1996).
 9. The Arizona site was at 34°N in high-elevation (2500 m) mixed conifer forests. This site is in the center of an extensive tract of forest with minimal human impact and containing large predators, including black bears, mountain lions, bobcats, coyotes, and foxes [T. E. Martin, *Ecology* 79, 653 (1998)]. The Argentina site was at 26°S in the center of El Rey National Park, a large park that contained large predators, including all large cats such as jaguars, mountain lions, and ocelots. The presence of large predators is important because their loss can allow increases in mesopredators that can increase nest predation rates (19).
 10. Nests were located using parental behavior and checked every 1 to 4 days to determine the fate of clutches and whether parents were successful in fledging at least one young or failed because of predation or other causes, following the method of T. E. Martin and G. R. Geupel [*J. Field Ornithol.* 64, 507 (1993)].
 11. A. F. Skutch, *Ornithol. Monogr.* 36, 575 (1985).
 12. P. Harvey and M. D. Pagel, *The Comparative Method in Evolutionary Biology* (Oxford Univ. Press, Oxford, 1991).
 13. Incubation was used for this test, because parents and young do not make noise during this period, allowing clear tests of the influence of parental activity. During the nestling period, the begging noise of young could influence predation rates independently of parental activity [D. Haskell, *Proc. R. Soc. London Ser. B* 257, 161 (1994); J. Briskie, P. R. Martin, T. E. Martin, *Proc. R. Soc. London Ser. B* 266, 2153 (1999)].
 14. J. J. Roper and R. R. Goldstein, *J. Avian Biol.* 28, 111 (1997).
 15. T. E. Martin, *Proc. Natl. Acad. Sci. U.S.A.* 85, 2586 (1988); *Nature* 380, 338 (1996).
 16. H. A. Ford, *Emu* 99, 91 (1991); R. E. Major et al., *Oikos* 69, 364 (1994); L. N. H. Taylor and H. A. Ford, *Wildl. Res.* 25, 587 (1998).
 17. A. F. Skutch, *Pacific Coast Avifauna* no. 34 (1960); *Publ. Nuttall Ornithol. Club* no. 7 (1967); *Publ. Nuttall Ornithol. Club* no. 10 (1972); *Publ. Nuttall Ornithol. Club* no. 19 (1981).
 18. T. B. Oatley, *Ostrich* 53, 206 (1982); R. A. Noske, *Emu* 91, 73 (1991); I. Rowley, M. Brooker, E. Russell, *Emu* 91, 197 (1991); A. Dyrce, *Emu* 94, 17 (1994).
 19. Y. Oniki, *Biotropica* 11, 60 (1979); J. P. Gibbs, *Oikos* 60, 155 (1993); J. Terborgh, *Ecology* 78, 1494 (1997).
 20. N. P. Ashmole, *Ibis* 103, 458 (1963); M. L. Cody, *Evolution* 20, 174 (1966); J. C. Z. Woinarski, *Proc. Ecol. Soc. Aust.* 14, 159 (1985); Y. Yom Tov, *Ibis* 136, 131 (1994).
 21. R. E. Ricklefs, *Proc. Natl. Acad. Sci. U.S.A.* 89, 4722 (1992).
 22. T. E. Martin and C. K. Ghalambor, *Am. Nat.* 153, 131 (1999).
 23. A. P. Møller and T. R. Birkhead, *Evolution* 48, 1089 (1994).
 24. A. Purvis and A. Rambaut, *Comp. Appl. Biosci.* 11, 247 (1995); T. E. Martin and J. Clobert, *Am. Nat.* 147, 1028 (1996).
 25. From 1993 to 1998, birds were videotaped during both incubation and nestling periods with video cameras for the first 6 hours of the day, beginning 0.5 hours before sunrise, as described in (22). This protocol standardized both time of day and sampling duration. All video recordings during the nestling period were made within 1 to 2 days of the time when primary feathers broke their sheaths to control for stage of development. The number of trips per hour was averaged over the 6 hours of monitoring for each nest (22).
 26. This study was designed to allow paired comparisons of traits between latitudes (Figs. 1 and 4) using paired sample *t* tests. Paired comparisons are a strong way to compare between latitudes because they can control for both phylogeny and ecology (Table 1). Paired comparisons use contrasts between extant species that do not require estimates of branch lengths and make no assumptions about modes of character evolution (12, 23). When phylogenetic paths cross, the average for nodes that do not cross is used (24). As a result, the two *Basileuterus* species are averaged and compared to the average of the two *Vermivora* species for all paired comparisons, yielding six paired comparisons.
 27. Visitation rates were quantified as described in (25). The number of trips per hour was calculated for each nest and then averaged across all nests within a species to obtain the mean for each species. A minimum of six nests (6 hours each) was used (22), but many more nests were sampled per species in most cases.
 28. Daily predation rates represent the probability per day that a nest is depredated [G. L. Hensler and J. D. Nichols, *Wilson Bull.* 93, 42 (1981)]. Only species with *n* > 20 nests were used.
 29. Relationships among species were examined while controlling for phylogeny by means of independent contrasts (3, 12). Controlling for phylogeny is important because behaviors may be similar in closely related species (12). A phylogeny was constructed using recent phylogenetic information (3). We calculated linear contrasts for each node in the phylogeny using the Comparative Analysis by Independent Contrast program [A. Purvis and A. Rambaut, *Comp. Appl. Biosci.* 11, 247 (1995)]. These independent contrasts were used to examine correlations that were forced through the origin (12).
 30. Food loading was measured as the size of visible food in the bills of parents arriving at the nest of nestlings that had broken their primary feather sheaths within 1 to 2 days. A small (4 cm) remote telephoto camera lens (MicroVideo) was placed within 1 m of nests to allow high-resolution closeup video images and measurement of food loading. The load size was estimated by measuring bill size and using it to calibrate the area of digital video images of load size obtained from video footage using GRABITIL. Area was used to estimate load size.
 31. Hole-nesting species typically have lower predation rates and larger clutches than do open-nesting birds (3). Five species in Argentina that nested in holes or in complex protected nests (*Piculus rubiginosus*, *Synallaxis superciliosa*, *Syndactyla rufosuperciliata*, *Troglodytes aedon*, and *Troglodytes solstitialis*) had daily predation rates from 0 to 0.018 (\bar{x} = 0.0066 ± 0.003), which is much lower than rates for the open-nesting species (Fig. 3B). However, we lacked clutch size data for three of these species.
 32. We thank C. Ghalambor, J. McKay, J. Tewksbury, K. Marchetti, T. Price, and two anonymous reviewers for helpful comments; many field assistants for their help in collecting the field data; the Arizona Game and Fish Agency and Coconino and Apache-Sitgreaves National Forests for their logistical support of the Arizona work; and the Laboratorio de Investigaciones Ecologicas de las Yungas, M. Rouges, P. Marconi, and El Rey National Park staff for logistical support of the Argentina work. Supported by grants from NSF (DEB-9527318, DEB-9707598, and DEB-9900343), the U.S. Geological Survey Biological Resources Division, and the International Program of the U.S. Fish and Wildlife Service.

7 October 1999; accepted 23 December 1999

Translocation of *C. elegans* CED-4 to Nuclear Membranes During Programmed Cell Death

Fangli Chen,^{1*}† Bradley M. Hersh,^{1*} Barbara Conradt,¹†
Zheng Zhou,¹ Dieter Riemer,² Yosef Gruenbaum,³
H. Robert Horvitz¹

The *Caenorhabditis elegans* Bcl-2-like protein CED-9 prevents programmed cell death by antagonizing the Apaf-1-like cell-death activator CED-4. Endogenous CED-9 and CED-4 proteins localized to mitochondria in wild-type embryos, in which most cells survive. By contrast, in embryos in which cells had been induced to die, CED-4 assumed a perinuclear localization. CED-4 translocation induced by the cell-death activator EGL-1 was blocked by a gain-of-function mutation in *ced-9* but was not dependent on *ced-3* function, suggesting that CED-4 translocation precedes caspase activation and the execution phase of programmed cell death. Thus, a change in the subcellular localization of CED-4 may drive programmed cell death.

Programmed cell death is important in regulating cell number and cell connections and for sculpting tissues during metazoan development (1). When misregulated, programmed cell death can contribute to various disease states, including cancer, autoimmune disease, and neurodegenerative disease (2). Many of the central components of the cell death machinery have been identified through genetic studies of the nematode *Caenorhabditis elegans* (3). Loss-of-function mutations in any of the genes *egl-1*, *ced-3*, or *ced-4* or a gain-of-function mutation in the gene *ced-9* block programmed cell death.

Loss-of-function mutations in *ced-9* cause sterility and maternal-effect lethality as a consequence of ectopic cell death and can be suppressed by *ced-3* and *ced-4* mutations but not by *egl-1* mutations, suggesting that *ced-9* acts upstream of *ced-3* and *ced-4* and downstream of *egl-1*. CED-9 is a member of the Bcl-2 family of cell-death regulators (4), and the EGL-1 protein contains a BH3 (Bcl-2 homology 3) domain and can physically interact with CED-9 (5). *ced-3* encodes a caspase (6), while CED-4 is similar to mammalian Apaf-1, an activator of caspases (7). CED-4 can bind

REPORTS

CED-9 and CED-3 in vitro, in yeast, and in mammalian cells (8), and the interaction of CED-9 and EGL-1 may influence CED-4 activity (9). These observations suggest a model (3) in which CED-3 causes programmed cell death; CED-4 activates CED-3; CED-4 is directly inhibited by CED-9 (10); and EGL-1 initiates cell death by directly inhibiting CED-9. To determine when and where these cell-death proteins act, we have explored physical interactions among them using immunohistochemistry.

To study the expression and subcellular localization of CED-9 and CED-4 in *C. elegans*, we generated polyclonal antibodies that recognize these proteins (11). Affinity-purified antibodies to CED-9 (anti-CED-9) specifically rec-

ognized bacterially expressed CED-9 and a 32-kD protein corresponding to CED-9 on a Western blot of wild-type (WT) (N2) embryo lysates; this protein was absent in *ced-9(n2812)* embryo lysates (12, 13). The *ced-9(n2812)* allele contains an amber stop mutation at codon 46 and is probably a molecular and genetic null allele (4). Fixed embryos stained with anti-CED-9 revealed that CED-9 was present in all cells during *C. elegans* embryogenesis (Fig. 1A), beginning as early as the two-cell stage. CED-9 levels peaked at approximately the 200-cell stage and slowly diminished, becoming undetectable around the time of hatching. CED-9 protein was not observed in larvae or adults. On the subcellular level, CED-9 exhibited a weblike, cytoplasmic staining pattern. CED-9 staining was highly similar to the staining of Mitotracker Red (14), which specifically labels mitochondria (Fig. 1).

Anti-CED-4 recognized bacterially expressed CED-4 and detected a 63-kD protein on Western blots of N2 embryo lysates; this protein was absent in *ced-4(n1162)* embryo lysates (12). The *ced-4(n1162)* allele contains an ochre stop mutation at codon 79 and is probably a molecular and genetic null allele (15). Embryos stained with anti-CED-4 displayed a weblike pattern in all cells (Fig. 1D), very similar to the patterns of CED-9 and

Mitotracker Red. CED-4 staining appeared at approximately the 100-cell stage, before the first programmed cell death, persisted through embryogenesis, and like CED-9, was not detected in larvae and adults. Of the 131 developmental cell deaths in *C. elegans* hermaphrodites, 113 occur during embryogenesis and the remainder occur during larval development. Although we have not detected CED-4 or CED-9 in larvae, *ced-4* and *ced-9* mutants are defective in larval programmed cell deaths, suggesting that the CED-4 and CED-9 proteins act postembryonically.

We examined whether the expression and localization of CED-9 and CED-4 were affected by mutations that disrupt programmed cell death. Loss-of-function mutations in *ced-3*, *ced-4*, and *egl-1*, genes required for programmed cell death, did not affect either the expression pattern or mitochondrial localization of CED-9 protein. The expression and localization of CED-4 protein was also unaffected by loss-of-function mutations in *ced-3* and *egl-1*. To determine the expression pattern and localization of CED-4 in the absence of functional CED-9 protein, we stained *ced-9(n2812)*; *ced-3(n717)* double-mutant embryos with anti-CED-4. Because *ced-9(n2812)* embryos derived from homozygous *ced-9(n2812)* hermaphrodites arrested before the appearance of visibly recognizable corpses and before CED-4 expression, these embryos could not be studied directly for CED-4 localization. Because *ced-3(n717)* did not affect the localization of CED-4 but does suppress the lethality of *ced-9(n2812)*, we instead used this double mutant to analyze CED-4 in the absence of CED-9. In *ced-9(n2812)*; *ced-3(n717)* embryos, CED-4 was not localized to mitochondria but rather was associated with nuclear membranes (Fig. 2, A to C), as visualized by double staining embryos with anti-CED-4 and antibodies directed against *C. elegans* lamin (16). We obtained similar results using the *ced-9* loss-of-function alleles *n1950 n2161* or *n1950 n2077* in combination with *ced-3(n717)*. Mitotracker Red staining was not altered in *ced-9(n2812)*; *ced-3(n717)* embryos, indicating that the shift in CED-4 localization represents a movement of CED-4 protein rather than a change in the morphology and/or localization of mitochondria (17).

To confirm this localization of CED-4 protein to nuclear membranes in *ced-9(lf)* embryos, we performed subcellular fractionations of embryo lysates (18). Both CED-9 and CED-4 were present predominantly in the organelle and membrane fraction, which includes the mitochondria [for example, (19)], in WT embryos (Fig. 3). By contrast CED-4 was present almost exclusively in the nuclear fraction in *ced-9(n2812)*; *ced-3(n717)* embryos. Thus, in WT embryos, in

¹Howard Hughes Medical Institute, Department of Biology, 68-425, Massachusetts Institute of Technology, Cambridge, MA 02139, USA. ²Department of Biochemistry, Max Planck Institute for Biophysical Chemistry, D-37016 Goettingen, Germany. ³Department of Genetics, Institute of Life Sciences, Hebrew University of Jerusalem, Jerusalem, 91904 Israel.

*These authors contributed equally to this work.

†Present address: Whitehead Institute, Department of Biology, W1-525, Massachusetts Institute of Technology, Cambridge, MA 02139, USA.

‡Present address: Max Planck Institute for Neurobiology, Am Klopferspitz 18A, D-82152 Planegg-Martinsried, Germany.

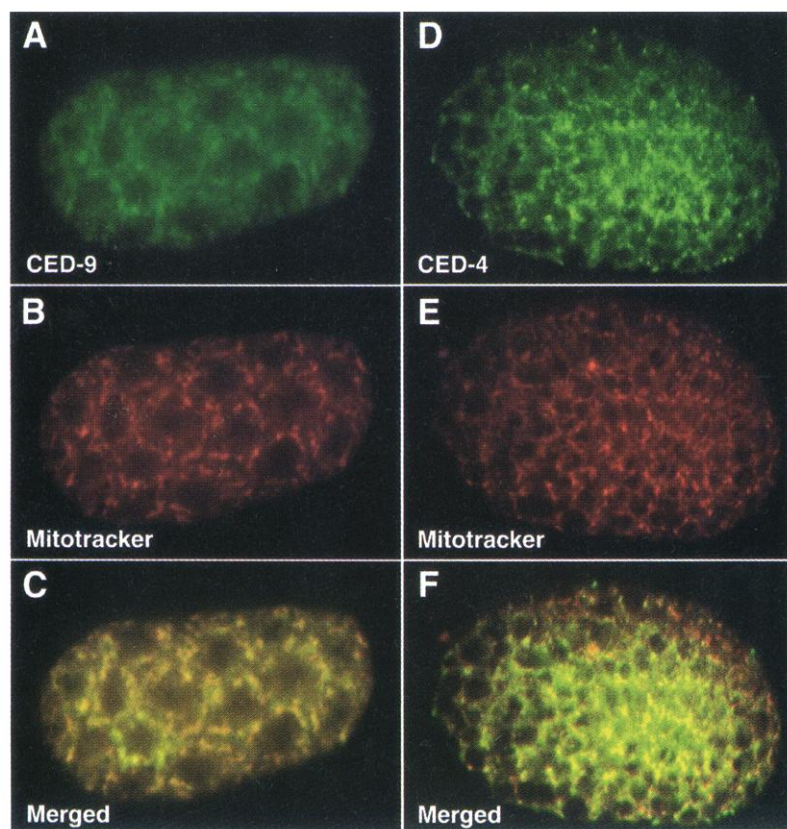


Fig. 1. CED-9 and CED-4 are localized to mitochondria in WT embryos. (A) CED-9 expression in a WT embryo of ~30 to 50 cells. (B) Mitotracker Red localization in the same embryo as in (A). (C) Merged image of (A) and (B). (D) CED-4 expression in a WT embryo of ~200 cells. (E) Mitotracker Red localization in embryo in (D). (F) Merged image of (D) and (E).

REPORTS

which most cells survive, both CED-9 and CED-4 appeared to be predominantly mitochondrial. However, in *ced-9(n2812); ced-3(n717)* embryos, in which ectopic cell death was presumably initiated but blocked by the *ced-3* mutation, CED-4 was redistributed from mitochondria to nuclei. Thus, CED-9 protein is necessary to localize CED-4 to mitochondria.

These data suggest that stimuli that induce programmed cell death would induce a redistribution of CED-4 to nuclear membranes and that it might be possible to block programmed cell death by blocking CED-4 relocalization. We tested these predictions by ectopically inducing programmed cell death in embryos.

The binding of EGL-1 protein to CED-9 may directly inhibit CED-9 function and trigger programmed cell death by releasing CED-4 from a CED-9–CED-4 complex (5, 9). To determine whether EGL-1 protein can affect the localization of CED-9 or CED-4, we expressed EGL-1 protein globally from an *egl-1* cDNA under the control of two *C. elegans* heat-shock promoters ($P_{hsp}egl-1$) (20) in the presence of the *ced-1(e1735)* mutation, which reduces cell corpse engulfment and allows the quantification of cells that have undergone programmed cell death (21). Animals carrying heat-shock vectors without the *egl-1* cDNA insert developed normally, but transgenic animals carrying $P_{hsp}egl-1$ arrested during embryogenesis after heat-shock treatment. The few hatched L1 larvae contained many more cell corpses than vector-only animals, indicating extensive programmed cell death (Table 1). Localization of CED-9 was unaffected in these animals. By contrast, overexpressed EGL-1 triggered the translocation of CED-4 from mitochondria to nuclei (Fig. 4A).

We next introduced the extrachromosomal array carrying $P_{hsp}egl-1$ into two strains in which programmed cell death is blocked. The *ced-3(n717)* mutation suppressed programmed cell death induced by EGL-1 overexpression (Table 1) but did not affect CED-4 translocation from mitochondria to nuclear membrane (22). This observation supports the idea that the release of CED-4 is not merely a consequence of cell death but rather precedes the execution of programmed cell death. Like *ced-3(n717)*, the *ced-9(n1950)* gain-of-function mutation blocked the ectopic death induced by *egl-1* overexpression (Table 1). However, unlike *ced-3(n717)*, *ced-9(n1950)* also blocked the translocation of CED-4 (Fig. 4B), suggesting that this mutant form of CED-9 either is unable to interact with EGL-1 or is unable to release CED-4. We tested the interaction of CED-9(G169E) protein, which is encoded by the *ced-9(n1950)* mutation, with EGL-1 protein both in vitro and in yeast two-hybrid experiments and were unable to detect any difference between the interactions of the

CED-9 and CED-9(G169E) proteins with the EGL-1 protein (23). It is possible that these in vitro studies failed to reveal a defect in the interaction between EGL-1 and CED-9 sufficient to produce the gain-of-function phenotype observed in vivo in *ced-9(n1950)* animals. Alternatively, in *ced-9(n1950)* animals, EGL-1 may form a ternary complex with CED-9 and CED-4 without causing the release of CED-4. We also generated an *egl-1* heat-shock con-

struct bearing the *egl-1(n3082)* mutation, which results in a truncated EGL-1 protein, a disruption of CED-9 binding, and a strong cell-death defective phenotype. Transgenic animals carrying this construct had significantly fewer corpses than animals bearing the WT *egl-1* construct (Table 1). CED-4 localization was predominantly mitochondrial, but in occasional animals a few cells displayed nuclear CED-4 localization. Thus, overexpression of this *egl-1(n3082)* gene resulted in a

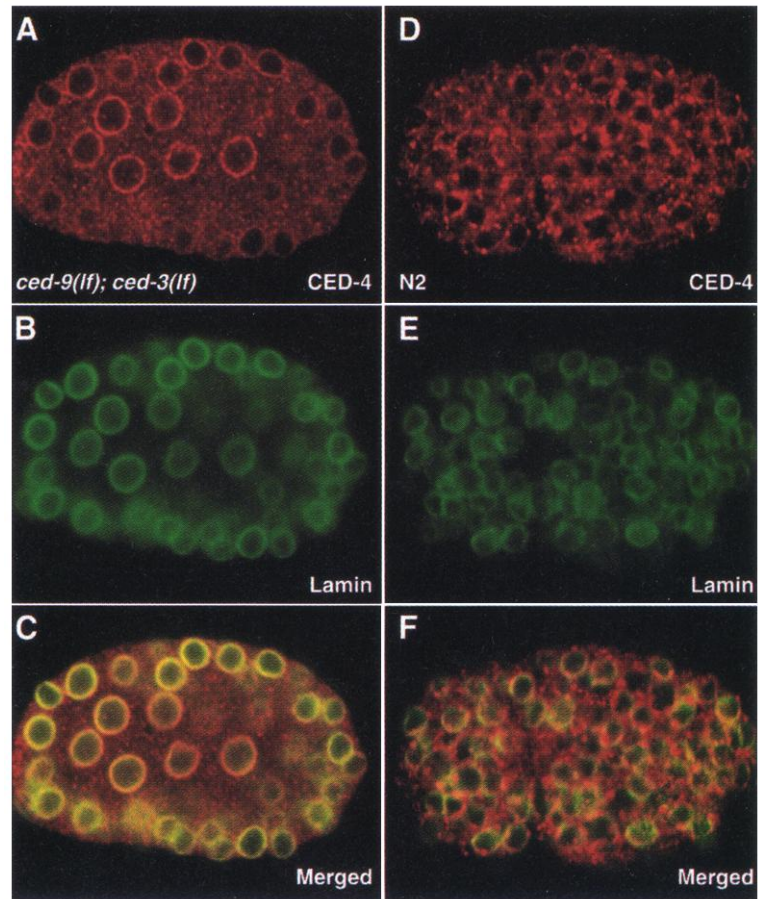
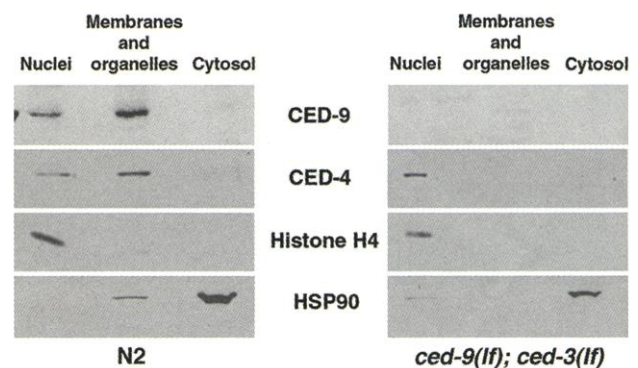


Fig. 2. CED-9 is required for the localization of CED-4 to mitochondria. (A) CED-4 expression in a *ced-9(n2812); ced-3(n717)* loss-of-function (*lf*) embryo of ~150 cells. (B) Lamin localization in the same embryo as in (A). (C) Merged image of (A) and (B). (D) CED-4 expression in WT embryo of ~200 cells. (E) Lamin staining of embryo in (D). (F) Merged image of (D) and (E).

Fig. 3. CED-4 fractionates primarily with membranes and organelles from WT embryos and with nuclei from *ced-9(lf)* embryos. Western blot of subcellular fractionation (18) of lysates from WT and *ced-9(n2812); ced-3(n717)* double-mutant embryos, separated into nuclear, organelle and membrane, and cytosolic fractions. Histone H4, a nuclear fraction marker. HSP90, *C. elegans* heat-shock protein, a cytosolic marker.



REPORTS

weak partial induction of both programmed cell death and CED-4 translocation.

Overexpression of *egl-1* was sufficient to trigger both cell death and CED-4 translocation. Is *egl-1* necessary for the CED-4 translocation that occurs in the absence of CED-9? We stained *ced-9(n2812)*; *ced-3(n717)*; *egl-1(n1084 n3082)* embryos and determined that CED-4 protein was nuclear, just as in the *ced-9(n2812)*; *ced-3(n717)* embryos. Thus, in the absence of CED-9 protein, EGL-1 is not required to release CED-4 from mitochondria to nuclei, indicating that EGL-1 promotes CED-4 translocation by antagonizing the activity of CED-9.

Thus, we observed that CED-4 was mitochondrial in living cells and nuclear in cells that had initiated programmed cell death, so that the subcellular localization of CED-4 appeared to correlate with the cell-death status of a cell. We next studied the localization of CED-4 in six *ced-4* missense mutants: *n2860*, *n2879*, *n3040*, *n3043*, *n3100*, and *n3141*. In five of the six mutants, CED-4 was mitochondrially localized in the presence of CED-9 and was associated with the nuclear membrane in the absence of CED-9, as in the WT. In *ced-4(n3040)* embryos, however, CED-4 displayed a diffuse, cytoplasmic localization both in the presence and in the absence of CED-9 (Fig. 4C), distinct from the weblike mitochondrial pattern of WT CED-

4. *ced-4(n3040)*, which causes a proline-to-leucine substitution at amino acid 23 (P23L) in a region that lacks any known protein motifs, results in as strong a cell-death defect as does *ced-4(n1162)*, which contains an early ochre nonsense mutation. This P23L substitution reduces the interaction between CED-9 and CED-4 by about 75% in the yeast two-hybrid assay (24). The failure of CED-4(P23L) to associate with either mitochondria or nuclear membranes suggests that CED-4 is actively recruited not only to mitochondria (presumably through interaction with CED-9) but also to the nucleus. Alternatively, CED-4 may first have to interact with CED-9 to be competent to translocate to nuclear membranes. That WT CED-4 associated with nuclear membranes in the absence of CED-9 argues against this latter model.

CED-9 localization to mitochondria in *C. elegans* embryos is not surprising, given that the mammalian CED-9-like cell-death protectors Bcl-2 and Bcl-X_L both localize to mitochondria (25). Although Bcl-X_L and the CED-4-like protein Apaf-1 have been reported to physically interact (26), Moriishi *et al.* (27) recently reported that they could find no interaction between Apaf-1 and any known anti-apoptotic Bcl-2 family member. Furthermore, there is no evidence for the localization of Apaf-1 to mitochondria. Apaf-1 was isolated as

a cytosolic activator of caspases (7), and overexpressed CED-4 is cytosolic in mammalian cells (8). Therefore, the mitochondrial localization of CED-4 is unexpected.

Our data suggest a model in which the activity of CED-4 is regulated by its subcellular localization. Specifically, we propose that in living cells, CED-9 prevents CED-4 activity by sequestering CED-4 to mitochondria. In cells triggered to undergo programmed cell death, EGL-1 binding to CED-9, possibly as a consequence of increased *egl-1* transcription (28), causes CED-4 release from CED-9 and allows the translocation of CED-4 to the nuclear region. There CED-4 activates the CED-3 procaspase, thereby causing programmed cell death.

How might we reconcile our findings with the report of Moriishi *et al.* (27) describing their failure to detect interactions between Apaf-1 and Bcl-2 family members? One possibility is that CED-9 has anti-apoptotic activity independent of its interaction with CED-4 and that this activity corresponds to the anti-apoptotic activity of Bcl-2 and Bcl-X_L. For example, CED-9 can directly inhibit the CED-3 caspase (29), although it has not been shown that this inhibition acts physiologically and the region of CED-9 involved is not present in Bcl-2 or Bcl-X_L. Furthermore, at least some CED-4 is localized to the nuclear membrane at the permissive temperature in *ced-9(n1653ts)* embryos (22), suggesting that this mutant CED-9 protein can protect against cell death even when CED-4 is localized to the nucleus; however, we suspect that the level of nuclear CED-4 in these embryos is lower than in cells that are dying, so this level may simply be insufficient to trigger programmed cell death.

The death-promoting proteins Bax and BAD, which like EGL-1 contain BH3 domains, translocate to mitochondria and bind anti-apoptotic Bcl-2 family members in response to apoptotic signals (30). Whether and how this translocation promotes cell death is unknown. Our results suggest that Bax and BAD may act to release Apaf-1 or another CED-4-like protein, allowing it to activate caspase processing. Some caspase precursors, specifically procaspases-2, and -3, are present in mitochondria and upon activation translocate to nuclei (31). It is possible that this movement of caspases involves the translocation of a complex that includes a CED-4-like protein. By analogy, the translocation of a CED-4-CED-3 complex from mitochondria to the nuclear envelope could provide access for the active caspase to both the nucleus and the cytosol, thereby fulfilling the roles of the multiple, differentially localized mammalian caspases.

The release of CED-4 from mitochondria resulted in the translocation of CED-4 to another distinct subcellular compartment rather than in the dispersal of CED-4 throughout the cell. This result, combined with our finding that the CED-

Table 1. EGL-1 induces ectopic cell death that can be suppressed by the *ced-9* gain-of-function mutation *n1950*. Corpses were counted in the heads of transgenic L1 animals subjected to heat shock (20) and represent the mean \pm SD and range observed (*n*, number of animals). The *egl-1(n1084 n3082)* allele is referred to as *egl-1(lf)*, whereas *egl-1(n3082)* indicates a transgene engineered to contain only the *n3082* 5-bp deletion and not the *n1084* lesion in the *egl-1* 3' regulatory region.

Genotype	Array	Number of corpses	Range	<i>n</i>
<i>ced-1</i> ; <i>egl-1(lf)</i>	Vector alone	0.4 \pm 0.6	0–2	15
<i>ced-1</i> ; <i>egl-1(lf)</i>	P _{hsp} <i>egl-1</i>	45.4 \pm 18.7	16–75	16
<i>ced-1</i> ; <i>ced-3</i> ; <i>egl-1(lf)</i>	P _{hsp} <i>egl-1</i>	0.5 \pm 0.7	0–2	15
<i>ced-1</i> ; <i>ced-9(n1950)</i> ; <i>egl-1(lf)</i>	P _{hsp} <i>egl-1</i>	1.3 \pm 1.3	0–4	15
<i>ced-1</i> ; <i>egl-1(lf)</i>	P _{hsp} <i>egl-1(n3082)</i>	4.4 \pm 3.2	0–13	20

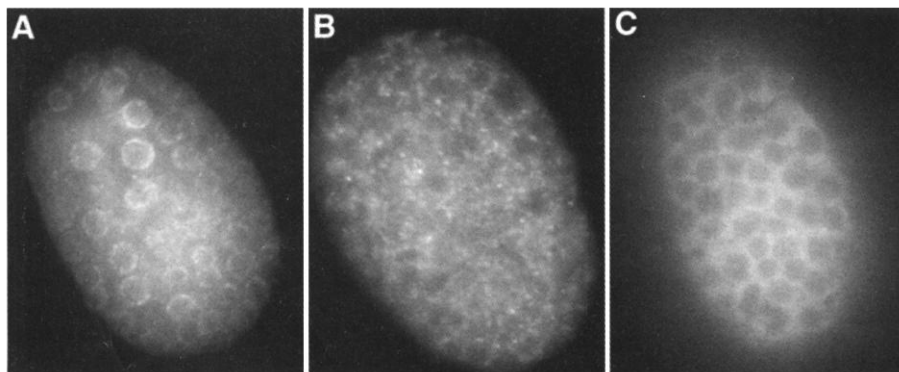


Fig. 4. Overexpression of EGL-1 induces CED-4 translocation from mitochondria to nuclear membranes in *ced-9(+)* embryos but not in *ced-9(n1950)* embryos. (A) CED-4 localization after heat shock in a *ced-9(+)* embryo carrying P_{hsp}*egl-1*. (B) CED-4 localization after heat shock in a *ced-9(n1950)* embryo carrying P_{hsp}*egl-1*. (C) CED-4 localization in a *ced-4(n3040)* embryo was diffusely cytoplasmic.

4(P23L) mutant protein was diffusely cytoplasmic, suggests that CED-4 is recruited to nuclear membranes, possibly by interacting with another protein or protein complex. The identification of such a CED-4 receptor should help us understand the mechanism of action of CED-4 in the execution of programmed cell death.

References and Notes

1. M. D. Jacobson, M. Weil, M. C. Raff, *Cell* **88**, 347 (1997).
2. C. B. Thompson, *Science* **267**, 1456 (1995).
3. M. M. Metzstein, G. M. Stanfield, H. R. Horvitz, *Trends Genet.* **14**, 410 (1998).
4. M. O. Hengartner and H. R. Horvitz, *Cell* **76**, 665 (1994).
5. B. Conradt and H. R. Horvitz, *Cell* **93**, 519 (1998).
6. J. Yuan et al., *Cell* **75**, 641 (1993).
7. H. Zou et al., *Cell* **90**, 405 (1997).
8. D. Wu, H. D. Wallen, G. Nuñez, *Science* **275**, 1126 (1997); M. Irmeler et al., *FEBS Lett.* **406**, 189 (1997); A. M. Chinnaiyan et al., *Science* **275**, 1122 (1997); M. S. Spector et al., *Nature* **385**, 653 (1997).
9. L. del Peso, V. M. Gonzalez, G. Nunez, *J. Biol. Chem.* **273**, 33495 (1998).
10. S. Seshagiri and L. K. Miller, *Curr. Biol.* **7**, 455 (1997).
11. A partial *ced-9* cDNA was cloned into vector pET19b to generate a His-10-CED-9 fusion protein lacking the COOH-terminal 29 amino acids of CED-9. The fusion protein was purified on Ni²⁺-nitrilotriacetic acid-agarose (Qiagen) and injected with RIBI adjuvant into rabbits. The antiserum was affinity-purified against His-10-CED-9 immobilized on nitrocellulose. For the generation of anti-CED-4, full-length *ced-45* cDNA was cloned into pXHA [S. J. Elledge et al., *Proc. Natl. Acad. Sci. U.S.A.* **89**, 2907 (1992)]. The hemagglutinin-CED-4 fusion was purified from inclusion bodies of *Escherichia coli* and injected into rabbits and rats. The rabbit antiserum was used without further purification, and rat antiserum was affinity-purified against glutathione-S-transferase-CED-4 immobilized on nitrocellulose. Embryos were collected by bleaching mixed-stage worms in a 0.8 N NaOH, 8% hypochlorite solution. Embryos were fixed and permeabilized essentially as described [C. Guenther and G. Garriga, *Development* **122**, 3509 (1996)]. Embryos were incubated in a 1:100 dilution of primary antibody, washed four times, incubated for 2 hours in a 1:25 dilution of secondary antibody, washed four times, washed once in phosphate-buffered saline plus 4',6'-diamidino-2-phenylindole (DAPI, 1 µg/ml), and resuspended in an equal volume of VECTASHIELD mounting medium (Vector Labs). Embryos for mitochondrial colocalization experiments were collected from worms grown in the dark on NGM agar plates containing MitoTracker Red CMXRos (2 µg/ml, Molecular Probes).
12. Supplementary data can be found in Web figure 1 at www.sciencemag.org/feature/data/1046764.shl.
13. Mutant strains carrying the following alleles of cell-death genes were used in this study: *ced-1(e1735)*, engulfment-defective; *ced-3(n717)*, splice acceptor mutation, exon 7; *ced-9(n2812)*, Q46amber; *ced-9(n1950)*, G169E; *ced-9(n1950 n2161)*, *ced-9(n1950 n2077)*, loss-of-function mutations; *ced-9(n1653)*, Y149N; *ced-4(n1162)*, Q79ochre; *ced-4(n2860)*, E263K; *ced-4(n2879)*, E276K; *ced-4(n3040)*, P23L; *ced-4(n3043)*, D20N; *ced-4(n3100)*, S339P; *ced-4(n3141)*, R53K; *egl-1(n1084)*, G-to-A nucleotide transition at nucleotide +5631; *egl-1(n1084 n3082)*, *n1084* lesion plus 5-base pair (bp) deletion in *egl-1* coding region.
14. M. Poot et al., *J. Histochem. Cytochem.* **44**, 1363 (1996).
15. J. Yuan and H. R. Horvitz, *Development* **116**, 309 (1992).
16. D. Riemer, H. Dodemont, K. Weber, *Eur. J. Cell Biol.* **62**, 214 (1993).
17. Supplementary data can be found in Web figure 2 at www.sciencemag.org/feature/data/1046764.shl.
18. Embryos for fractionation were collected as described (17). Embryos were resuspended in five volumes of cold hypotonic buffer (10 mM KCl, 1.5 mM MgCl₂, 1 mM

- EDTA, 1 mM EGTA, 1 mM dithiothreitol, 0.1 mM phenylmethylsulfonyl fluoride, 250 mM sucrose) and homogenized in a 1-ml Dounce tissue grinder. The homogenates were centrifuged at 40g briefly to remove worm debris. The supernatant was centrifuged twice at 750g for 10 min, and the resulting pellets were pooled as the nuclear fraction. The supernatant was further centrifuged at 100,000g for 1 hour. The pellet was designated the organelle and membrane fraction and the supernatant the soluble cytosolic S100 fraction. The pooled nuclear fraction was washed once with homogenization buffer. One-fifth of each fraction was used for immunoblotting analysis. Rabbit polyclonal antibody directed against human acetylated histone H4 (Upstate Biotechnology) was used as a marker for the nuclear fraction. Monoclonal anti-Ce HSP90 was used as a marker for the cytosolic fraction.
19. D. D. Newmeyer, D. M. Farschon, J. C. Reed, *Cell* **79**, 353 (1994).
20. *P_{hsp} egl-1 (5)* was injected at a concentration of 2 ng/µl, along with p76-16B [L. Bloom and H. R. Horvitz, *Proc. Natl. Acad. Sci. U.S.A.* **94**, 3414 (1997)] at 50 ng/µl, into a *ced-1(e1735)*; *egl-1(n1084 n3082) unc-76(e911)* strain as described [C. Mello and A. Fire, *Methods Cell Biol.* **48**, 451 (1995)]. For immunofluorescence, mixed-stage transgenic worms were incubated at 33°C for 1 hour followed by a 2-hour recovery at 20°C. Embryos were then collected as in (17). For analysis of cell corpses, transgenic adults were allowed to lay eggs at 20°C for 2 hours, subjected to a 1-hour heat shock at 33°C, allowed to lay eggs for an additional 2 hours at 20°C, and then removed from the plates. Hatched L1 transgenic animals were examined by Nomarski microscopy for corpses in the head.
21. E. M. Hedgecock, J. E. Sulston, J. N. Thomson, *Science* **220**, 1277 (1983).

22. F. Chen, B. M. Hersh, H. R. Horvitz, data not shown.
23. B. M. Hersh, B. Conradt, H. R. Horvitz, data not shown.
24. S. Otililie et al., *Cell Death Differ.* **4**, 526 (1997).
25. M. Nguyen et al., *J. Biol. Chem.* **268**, 25265 (1993); Y. Akao et al., *Cancer Res.* **54**, 2468 (1994); S. Krajewski et al., *Cancer Res.* **53**, 4701 (1993).
26. G. Pan, K. O'Rourke, V. M. Dixit, *J. Biol. Chem.* **273**, 5841 (1998); Y. Hu et al., *Proc. Natl. Acad. Sci. U.S.A.* **95**, 4386 (1998).
27. K. Moriishi et al., *Proc. Natl. Acad. Sci. U.S.A.* **96**, 9683 (1999).
28. B. Conradt and H. R. Horvitz, *Cell* **98**, 317 (1999).
29. D. Xue and H. R. Horvitz, *Nature* **390**, 305 (1997).
30. K. G. Wolter et al., *J. Cell Biol.* **139**, 1281 (1997).
31. S. A. Susin et al., *J. Exp. Med.* **189**, 381 (1999); M. Mancini et al., *J. Cell Biol.* **140**, 1485 (1998); B. Zhivotovsky, A. Samali, A. Gahm, S. Orrenius, *Cell Death Differ.* **6**, 644 (1999).
32. We thank members of the Horvitz laboratory for helpful comments and discussions concerning this manuscript. We thank Y. Yamaguchi and J. Miwa for anti-Ce HSP90 monoclonal antibody; D. Xue for generating pET19b-CED-9ΔC; B. Davies, A. Madi, S. Shaham, E. Speliotes, and G. Stanfield for *ced-4* missense mutations; B. Castor for DNA sequence determinations; and M. Boxem and S. van den Heuvel for assistance with microscopy. B.M.H. was supported by a Howard Hughes Predoctoral Fellowship. B.C. was supported by a postdoctoral fellowship from the Jane Coffin Childs Memorial Fund for Medical Research and a Leukemia Society Special Fellowship. Z.Z. was supported by a Cancer Research Fund of the Damon Runyon-Walter Winchell Foundation Fellowship (DRG 1343). H.R.H. is an Investigator of the Howard Hughes Medical Institute.

2 November 1999; accepted 12 January 2000

Regulation of Cell Fate Decision of Undifferentiated Spermatogonia by GDNF

Xiaojuan Meng,¹ Maria Lindahl,^{2*} Mervi E. Hyvönen,^{1*} Martti Parvinen,⁵ Dirk G. de Rooij,⁶ Michael W. Hess,³ Anne Raatikainen-Ahokas,¹ Kirsi Sainio,¹ Heikki Rauvala,⁴ Merja Lakso,⁴ José G. Pichel,⁷ Heiner Westphal,⁸ Mart Saarma,² Hannu Sariola^{1†}

The molecular control of self-renewal and differentiation of stem cells has remained enigmatic. Transgenic loss-of-function and overexpression models now show that the dosage of glial cell line-derived neurotrophic factor (GDNF), produced by Sertoli cells, regulates cell fate decisions of undifferentiated spermatogonial cells that include the stem cells for spermatogenesis. Gene-targeted mice with one *GDNF*-null allele show depletion of stem cell reserves, whereas mice overexpressing GDNF show accumulation of undifferentiated spermatogonia. They are unable to respond properly to differentiation signals and undergo apoptosis upon retinoic acid treatment. Nonmetastatic testicular tumors are regularly formed in older GDNF-overexpressing mice. Thus, GDNF contributes to paracrine regulation of spermatogonial self-renewal and differentiation.

The stem cells for spermatogenesis are single cells in the periphery of seminiferous tubules. The stem cells either self-renew by forming single stem cells or they become interconnected pairs of cells destined to differentiate. Such cells divide further into syncytial chains of usually not more than 16 cells that enter mitosis and apoptosis synchronously (1, 2).

Stem cells, pairs, and chains are collectively called undifferentiated spermatogonia, which subsequently become differentiating spermatogonia, spermatocytes, spermatids, and sperm cells. All types of undifferentiated spermatogonia are morphologically and molecularly alike, but they can be distinguished by the absence or presence of synchronized mitotic